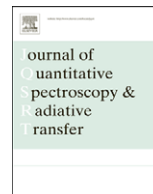




Contents lists available at ScienceDirect

Journal of Quantitative Spectroscopy & Radiative Transfer

journal homepage: www.elsevier.com/locate/jqsrt

Spectral scattering properties of a nanohole in a noble-metal film in the evanescent waves area

Elena Eremina^{a,*}, Yuri Eremin^{b,1}, Natalia Grishina^{b,1}, Thomas Wriedt^{c,2}^a *Universitaet Bremen, Badgasteiner Str. 3, 28359 Bremen, Germany*^b *Moscow Lomonosov State University, Lenin's Hills, 119991 Moscow, Russia*^c *Institut für Werkstofftechnik, Badgasteiner Str. 3, 28359 Bremen, Germany*

ARTICLE INFO

Article history:

Received 20 November 2008

Received in revised form

12 January 2009

Accepted 15 January 2009

Keywords:

Spectral properties

Evanescent wave

Nanohole

Extreme transmission

Discrete sources method

Plasmon resonance

ABSTRACT

The effect of enhanced optical transmission through subwavelength holes and their arrays is used for multiple practical applications especially in optical antennas and local biosensors design. This effect is usually considered under excitation of plane wave propagating at the normal direction to the screen surface. In this work the effect of extreme transmission through the hole in the evanescent wave's area is in focus. The discrete sources method has been applied to analyse the spectral characteristics of light scattered by a cylindrical nanohole in a noble-metal film on a prism surface. The influence of the wavelength, incident angle, film materials and hole's filling on the scattering characteristics has been investigated. A close correlation between the effect of extreme transmission and the surface plasmon resonances has been detected.

© 2009 Elsevier Ltd. All rights reserved.

1. Introduction

Since the effect of enhanced optical transmission through arrays of subwavelength holes in metal screens was discovered by Ebbesen et al. [1] it has attracted considerable interest by numerous researchers. The ability to localize light in spots much smaller than the volume predicted by diffraction theory offers multiple practical applications in nanooptics and biophotonics. The effect of extraordinary transmission (EOT) appears at a certain wavelength of the incident light, which depends on the film's material and has been detected for single holes as well as for arrays of holes [2]. In the paper of Wannemacher [3] this effect has been explained by plasmon excitation. It is now generally agreed that surface plasmon resonance (SPR) plays a key role in the enhancement of light transmission through sub-wavelength apertures in noble-metal screens [2,4]. Recently, several teams of researchers worldwide have examined the transmission properties of subwavelength apertures in connection with the development of optical antennas and biosensors [5–8].

In the recent paper [9] the effect of extreme light transmission through a nanohole in a noble-metal film on the prism surface has been described. The extreme transmission effect (ETE) differs from the EOT by several aspects. It appears in the evanescent wave area only and it does not depend on film thickness, hole's diameter and its filling. Extreme transmission means that the transmission cross-section (TCS) under an "optimal angle" beyond the critical one (in the evanescent wave area) exceeds an order of the TCS under normal excitation, which as a rule is used for the EOT demonstration.

* Corresponding author. Tel.: +49 421 218 3583; fax: +49 421 218 5378.

E-mail addresses: eremina@iwt.uni-bremen.de (E. Eremina), eremin@cs.msu.su (Y. Eremin), thw@iwt.uni-bremen.de (T. Wriedt).¹ Tel./fax: +7 095 939 1776.² Tel.: +49 421 218 3583; fax: +49 421 218 2507.

In this paper the discrete sources method (DSM) has been adjusted to calculate spectral characteristics of light scattered by a nanohole in a metal film on a glass prism. It is shown that the ETE appears at different wavelengths, but is especially pronounced at the wavelength where the TCS reaches its maximum value.

Moreover, it has been found that this maximum is achieved for a real part of the wavelength depending on the film permittivity falls within the range $[-11.5, -10.2]$. This can be used to produce appropriate film materials enhancing the effect of extreme light transmission. Also a close connection of the ETE to the SPR [10] has been detected.

As it is the second paper on this topic, the major part of DSM theory has been omitted and just the key features relating to the solution to the scattering problem is provided. A reader can find the detailed theory in a recently published paper [9]. In the following chapter brief outlines of the DSM are given. In the third chapter numerical results are presented and discussed.

2. Scattering problem statement and DSM outlines

Let the whole space be divided into three areas (see also Fig. 1): air D_0 , film D_f and a glass prism D_1 . Let the plane Σ_1 separate film and glass prism and the plane Σ_f air and film. An axially symmetric hole occupying a certain domain D_i with a smooth boundary ∂D is situated inside the film of thickness d and bounded by the planes Σ_1 and Σ_f . We assume that the symmetry axis of the hole coincides with the normal direction to Σ_1 .

A Cartesian coordinate system $Oxyz$ is introduced by choosing its origin O at the prism-surface Σ_1 in the centre of the hole's bottom. The Oz axis coincides with the symmetry axis of the hole and is directed into D_0 . The plane $z = 0$ corresponds to the Σ_1 plane (Fig. 1).

Let us assume the exciting field $\{\mathbf{E}^0, \mathbf{H}^0\}$ is a plane wave propagating from the prism domain D_1 at the angle θ_1 with respect to the z -axis. First, the plane wave $\{\mathbf{E}^0, \mathbf{H}^0\}$ scattering problem on the layered media is solved. The result yields external excitation fields $\{\mathbf{E}_\zeta^0, \mathbf{H}_\zeta^0\}$, $\zeta = 0, f, 1$ in the domains $D_{0f,1}$, which satisfy the transmission conditions at the plane interfaces Σ_{1f} . While in D_{1f} the total field consists of incident and reflected waves, in D_0 the total field includes the transmitted wave which transforms to an evanescent one beyond the critical angle.

In particular, the exciting field inside the film can be represented by a linear combination of the plane waves transmitted through Σ_1 and that reflected from Σ_f :

$$\mathbf{E}_f^0 = W_i^{P,S} \mathbf{E}_f^{(+),P,S} + W_r^{P,S} \mathbf{E}_f^{(-),P,S}, \quad \mathbf{H}_f^0 = W_i^{P,S} \mathbf{H}_f^{(+),P,S} + W_r^{P,S} \mathbf{H}_f^{(-),P,S}, \quad (1)$$

where

$$\mathbf{E}_f^{(\pm),P} = (\mp \cos \theta_f \mathbf{e}_x + \sin \theta_f \mathbf{e}_z) \gamma^\pm, \quad \mathbf{H}_f^{(\pm),P} = -n_f \mathbf{e}_y \gamma^\pm,$$

$$\mathbf{H}_f^{(\pm),S} = n_f (\mp \cos \theta_f \mathbf{e}_x + \sin \theta_f \mathbf{e}_z) \gamma^\pm, \quad \mathbf{E}_f^{(\pm),S} = \mathbf{e}_y \gamma^\pm,$$

$$\gamma^\pm = \exp\{-jk_f(x \sin \theta_f \pm z \cos \theta_f)\}, \quad k_\zeta^2 = k^2 \varepsilon_\zeta \mu_\zeta, \quad n_\zeta = \sqrt{\varepsilon_\zeta \mu_\zeta}, \quad \zeta = 0, f, 1,$$

$$W_i^{P,S} = \frac{T_{1f}^{P,S}}{1 - R_{f1}^{P,S} R_{f0}^{P,S} e_f^2}, \quad W_r^{P,S} = -R_{f0}^{P,S} e_f^2 W_i^{P,S}, \quad e_f = \exp\{-jk_f d \cos \theta_f\}.$$

Here $R_{\alpha\beta}^{P,S}$, $T_{\alpha\beta}^{P,S}$ are the corresponding reflection and transmission coefficients of the interface between D_α and D_β , for P- and S-polarized plane waves [11], $\varepsilon_\zeta, \mu_\zeta$ the permittivity and permeability of the corresponding media, $k = \omega/c$, θ_f is the transmission angle according to Snell's law, $\mathbf{e}_{x,y,z}$ is an orthogonal basis function.

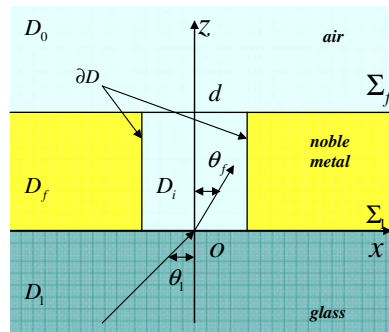


Fig. 1. Illustration of the model's geometry: a cylindrical nanohole in a metal film on a glass prism.

Then the mathematical statement of the scattering problem for the scattered field outside D_i and the total field inside D_i can be formulated as follows:

$$\begin{aligned} \nabla \times \mathbf{H}_\zeta &= jk\varepsilon_\zeta \mathbf{E}_\zeta, \quad \nabla \times \mathbf{E}_\zeta = -jk\mu_\zeta \mathbf{H}_\zeta \quad \text{in } D_\zeta, \quad \zeta = 0, 1, f, i, \\ \mathbf{n}_p \times (\mathbf{E}_i(p) - \mathbf{E}_f(p)) &= \mathbf{n}_p \times \mathbf{E}_f^0(p), \\ \mathbf{n}_p \times (\mathbf{H}_i(p) - \mathbf{H}_f(p)) &= \mathbf{n}_p \times \mathbf{H}_f^0(p), \quad p \in \partial D, \\ \mathbf{e}_z \times (\mathbf{E}_f(p) - \mathbf{E}_1(p)) &= 0, \quad \mathbf{e}_z \times (\mathbf{E}_0(p) - \mathbf{E}_f(p)) = 0, \\ \mathbf{e}_z \times (\mathbf{H}_f(p) - \mathbf{H}_1(p)) &= 0, \quad \mathbf{e}_z \times (\mathbf{H}_0(p) - \mathbf{H}_f(p)) = 0, \quad p \in \sum_f \end{aligned} \quad (2)$$

and radiation/attenuation conditions at infinity for the scattered field in $D_{0,1}$ and in D_f .

Here, \mathbf{e}_z is the unit normal vector to the planes $\Sigma_{1,f}$, \mathbf{n}_p is the outward unit normal vector to ∂D , $k = \omega/c$. If $\text{Im } \varepsilon_\zeta, \mu_\zeta \leq 0$ (the time dependence for the fields is chosen as $\exp[j\omega t]$) and the particle surface is smooth enough ($\partial D \in C^{2,\alpha}$), then the above boundary value scattering problem is uniquely solvable [12].

After the plane wave $\{\mathbf{E}^0, \mathbf{H}^0\}$ scattering problem at the interface has been solved, the approximate solution to the boundary value problem (2) for the scattered field $\{\mathbf{E}_\zeta, \mathbf{H}_\zeta\}$ in D_ζ , $\zeta = 0, f, 1$ and the total field $\{\mathbf{E}_i, \mathbf{H}_i\}$ in D_i is constructed. Let us remember that the boundary conditions of problem (2) are inhomogeneous at the hole's surface only.

To construct an approximate solution the DSM [13] is employed. In the frame of DSM the approximate solution is constructed by representing the electromagnetic fields as a finite linear combination of electric and magnetic fields of multipoles distributed over the axis of symmetry inside the hole or in adjoint complex plane. Besides, the fields analytically satisfy the transmission conditions enforced at the plane interfaces $\Sigma_{1,f}$, which provides an opportunity to account for whole interactions between hole and interfaces occurring due to multiple field reflections. Then the approximate solution satisfies the Maxwell equations in the domains D_ζ , $\zeta = 0, 1, f, i$, the infinity conditions and the transmission conditions at the plane interfaces $\Sigma_{1,f}$. Thus, the scattering problem is reduced to a problem of an approximation of the exciting field on the holes surface ∂D . Finally, the amplitudes of the discrete sources (DS) are to be determined from the boundary conditions enforced at ∂D (see (2)).

To construct the fields of dipoles and multipoles that analytically satisfy the transmission conditions at the plane interfaces $\Sigma_{1,f}$, Green's tensor for a layered interface is used [14]. An approximate solution to the scattering problem is constructed taking into account the rotational symmetry of the scattering problem geometry (a hole together with a layered interface) as well as the polarization of the exciting field [13]. A detailed description of the method, including all related representations can be found in [9]. The completeness of the system of multipoles guarantees the convergence of the approximate solution to the exact one [15].

The approximate solution based on DSM satisfies all the conditions of the scattering problem (2) except the transmission conditions at the hole's surface ∂D . These conditions are used to determine the unknown amplitudes of DS. Since the scattering problem geometry is axially symmetric with respect to the z -axis and the DS are distributed over the axis of symmetry, fulfilling the transmission conditions (2) at the surface ∂D can be reduced to a sequential set of 1D transmission problems for the Fourier harmonics of the fields. Hence, instead of matching the fields on the scattering surface ∂D , their Fourier harmonics are matched separately by reducing the approximation problem on the surface ∂D to a set of 1D problems enforced at the particle surface generatrix \mathfrak{A} . By solving these problems one can determine the DS amplitudes.

For the evaluation of the amplitudes various numerical schemes have been suggested. It has been found that more stable results can be obtained by using the generalized point-matching technique and a pseudo-solution to corresponding over-determined system of linear equations [16]. DSM is a direct method and therefore it allows solving the scattering problem for the entire set of incident angles θ_1 and for both polarizations (P and S) at once. Besides, the DSM numerical scheme provides an opportunity to control the actual convergence of the approximate solution to the exact one by a posterior error estimation [13].

After the amplitudes of the DS have been determined, one can calculate the far field pattern $\mathbf{E}_\infty(\theta, \varphi)$ of the scattered field, which is determined at the upper semi-sphere $\Omega = \{0^\circ \leq \theta \leq 90^\circ, 0^\circ \leq \varphi \leq 360^\circ\}$ and is given by

$$\mathbf{E}_0(M)/|\mathbf{E}^0(z=0)| = \frac{\exp\{-jk_0 r\}}{r} \mathbf{E}_\infty(\theta, \varphi) + o(r^{-1}), \quad z > d, \quad r = |M| \rightarrow \infty.$$

After asymptotical estimation of the Weyl–Sommerfeld integrals involved in the representation for the approximate solution [16], the components of the far field patterns for P/S polarization can be represented as finite linear combinations of elementary functions. This ensures low computational efforts for the analysis of the scattering characteristics in the far zone.

3. Numerical results and discussion

The differential scattering cross-section (DSC) is calculated as:

$$I^{P,S}(\theta_1, \theta, \varphi) = |E_{\infty, \theta}^{P,S}(\theta_1, \theta, \varphi)|^2 + |E_{\infty, \varphi}^{P,S}(\theta_1, \theta, \varphi)|^2, \quad (3)$$

where $E_{\infty, \theta, \varphi}^{P,S}$ ($\theta_1, \theta, \varphi$) are the components of the far field pattern for a P and S polarized incident wave in a spherical coordinate system θ, φ [10].

Here the TCS is considered, which represents the integrated intensity transmitted into the upper semi-sphere $\Omega = \{0^\circ \leq \theta \leq 90^\circ, 0^\circ \leq \varphi \leq 360^\circ\}$:

$$\sigma^{P,S}(\theta_1) = \int_{\Omega} I^{P,S}(\theta_1, \theta, \varphi) d\omega \quad (4)$$

Next, some numerical results obtained using the DSM model are presented and discussed. In the recent paper [9] the dependence of the transmitted intensity on the incident angle has been examined. In this paper spectral characteristics of the transmitted light are in focus. The scattering properties of a hole with diameter $D = 35$ nm in a film of thickness $d = 50$ nm excited by a light source with a wavelength in the range of $\lambda = 400$ – 700 nm are considered. For the film materials mostly silver (Ag) and gold (Au) have been taken. In some results copper (Cu) and platinum (Pt) have been used as well. Refractive indices of the film and prism materials have been taken from the paper of Lynch and Hunter [17].

In Fig. 2 the curves for TCS (4) versus wavelength for different incident angles $\theta_1 = 0^\circ, 42^\circ, 44^\circ$ are presented for a hole in an Ag film. One can see, that while four of five curves for S-polarized external excitation monotonically decrease, the curve for P-polarized light for $\theta_1 = 44^\circ$ has a maximum at about $\lambda = 532$ nm ($\text{Re } \epsilon_r(\text{Ag}) \cong -10.2$). The incident angle $\theta_1 = 44^\circ$ is beyond the critical angle $\theta_c = 41.2^\circ$, and therefore in the area where the evanescent wave appear in D_0 . In Fig. 3 the TCS versus incident angle is presented for the same hole in Ag and Au films for both polarizations for a fixed wavelength $\lambda = 532$ nm. Here we observe that while the S-polarized curves monotonically decrease the curves for P-polarization first drop down and then rapidly jump up two orders in value in the vicinity of critical angle. This effect of extreme transmission of the scattered light seems to be stronger for a silver film, than for a gold one.

In Fig. 4 results similar to those presented in Fig. 2 are given for the case of an Au film. Here we see, that the curves demonstrate quite similar behaviour except the curve for P-polarized light under $\theta_1 = 44^\circ$ which has a distinct maximum at $\lambda = 670$ nm ($\text{Re } \epsilon_r(\text{Au}) \cong -11.5$). In Fig. 5 the TCS versus incident angle is presented for the hole in Ag and Au films for both polarizations for $\lambda = 670$ nm. This time the effect of extreme transmission is stronger for the Au film. This result could be expected because in this case the wavelength has been chosen corresponding to the maximum values for an Au film.

Next, just P-polarized light is considered, as S-polarization does not show the distinct behaviour that can be observed for P polarization. To investigate the influence of the film parameters on the spectral behaviour of the TCS, Fig. 6 shows the results for TCS versus wavelength for P-polarized excitation for the same hole in films of different materials. Together with gold and silver, copper (Cu) and platinum (Pt) are taken as film materials. From Fig. 6 one can see that three materials demonstrate at least one maximum in the considered wavelength range, only Pt demonstrates simple monotonic behaviour. For a Cu film the maximum value is achieved at $\lambda = 630$ nm ($\text{Re } \epsilon_r(\text{Cu}) \cong -11.5$). Compared to the other materials Ag demonstrates the highest peak. In Fig. 7 the TCS versus incident angle for the same film materials is presented for a wavelength $\lambda = 532$ nm. One sees that all materials demonstrate a jump in the vicinity of the critical angle but the magnitude of the maximum is distributed in accordance with the value of the maximum values from Fig. 6. For example Pt together with other materials shows a sharp minimum at about $\theta_1 = 44^\circ$ but then unlike other materials its TCS-curve leaps up to a value just a bit higher than values it had before the minimum. The most obvious effect of extreme transmission appears for Ag and Au.

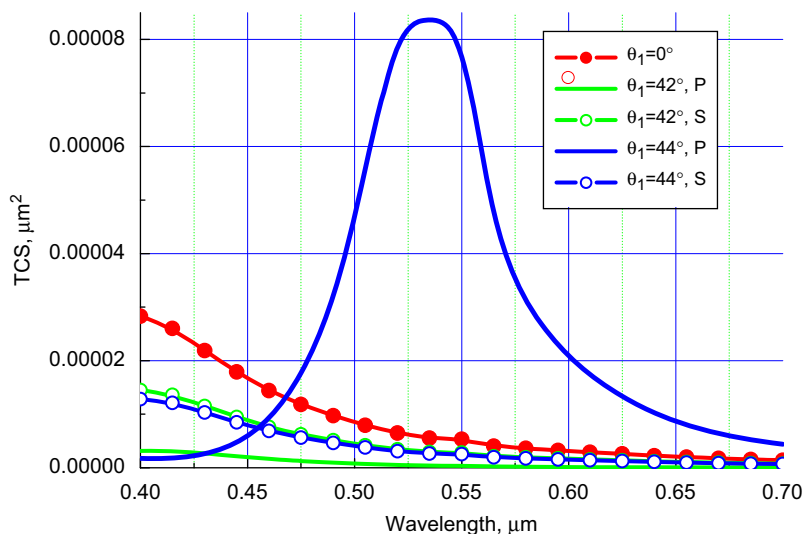


Fig. 2. Transmission cross-section (TCS) (4) for a cylindrical hole $D = 35$ nm, in Ag film $d = 50$ nm, on a glass prism.

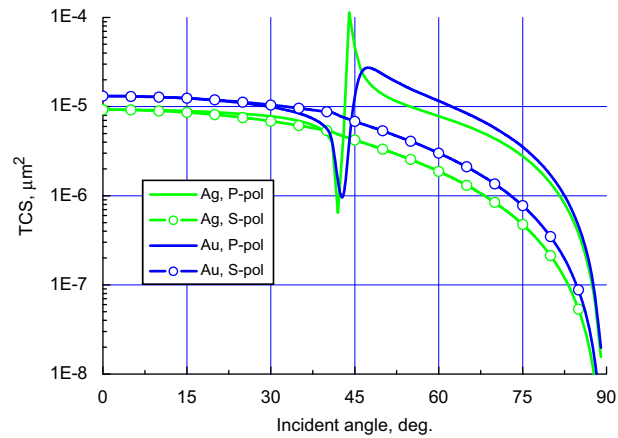


Fig. 3. TCS for holes in Ag and Au films on a glass prism, $\lambda = 532$ nm.

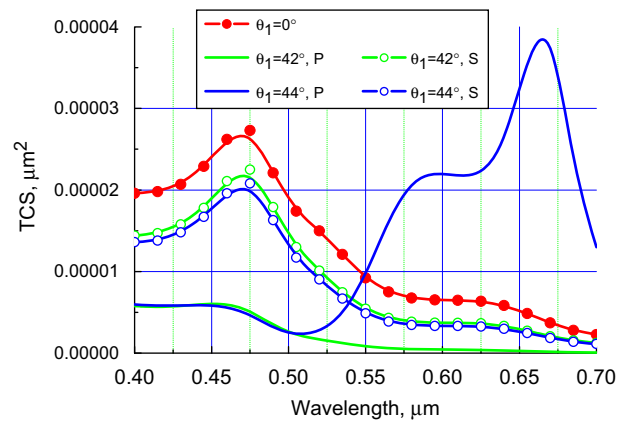


Fig. 4. TCS for a hole in Au film on a glass prism.

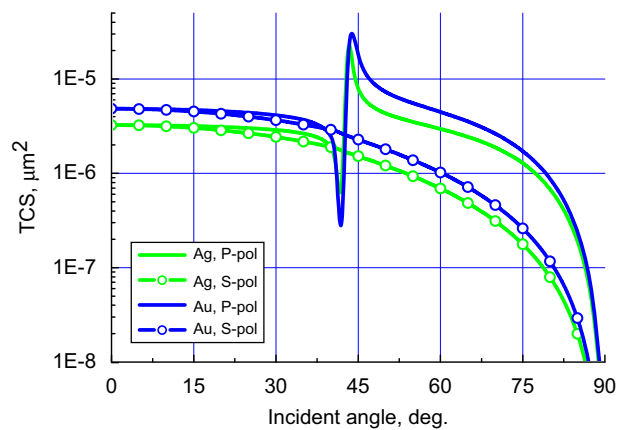


Fig. 5. TCS for holes in Ag and Au films on a glass prism, $\lambda = 670$ nm.

Let us now analyse the influence of evanescent waves on the transmission effect. Evanescent waves appear in the media with lower refractive index when the incident angle exceeds the critical one: $\theta_c = \arcsin(n_0/n_1)$. To check if evanescent waves are really important for the ETE, now different prism D_1 materials be considered: glass with a refractive index $n_1 = 1.52$ ($\theta_c \cong 41.2^\circ$), SiN with $n_1 = 2.034$ ($\theta_c = 29.4^\circ$) and air with $n_1 = 1.0$. In the cases of glass and SiN the area of

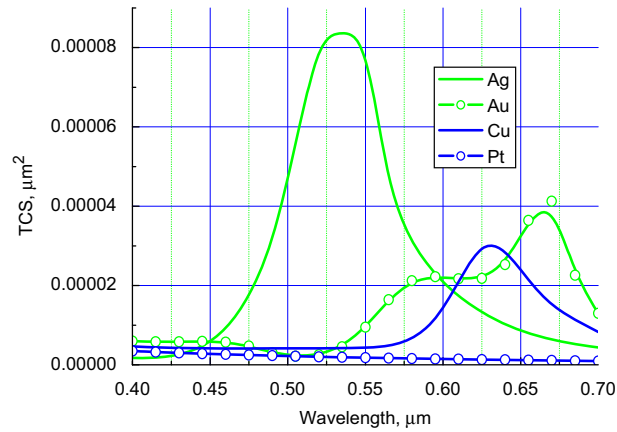


Fig. 6. TCS for holes in films of different materials under $\theta_1 = 44^\circ$, P-polarization.

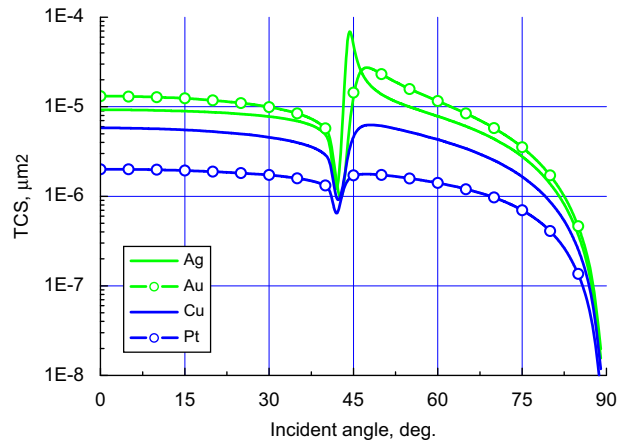


Fig. 7. TCS for holes in films of different materials, P-polarization, $\lambda = 532$ nm.

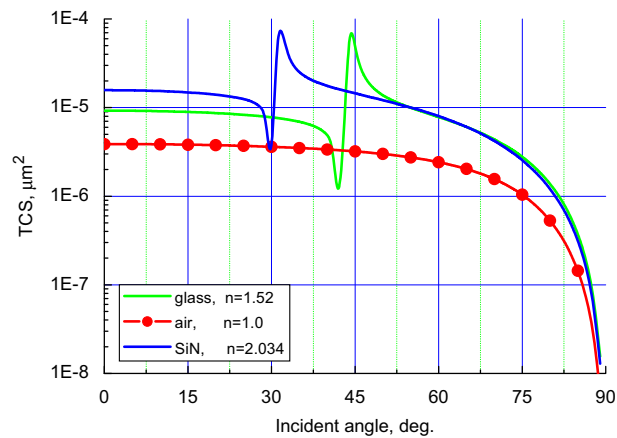


Fig. 8. TCS for a hole in Ag film, P-polarization, $\lambda = 532$ nm, different prism materials.

evanescent waves appears beyond the according critical angles. In case of air in D_1 there are no evanescent waves as D_1 and D_0 will have the same refractive index.

In Fig. 8 the TCS versus incident angle for the same hole in an Ag film is presented for different prism materials at $\lambda = 532$ nm. From the computed results one can see that in the case of air (no evanescent waves appear) the curve has a

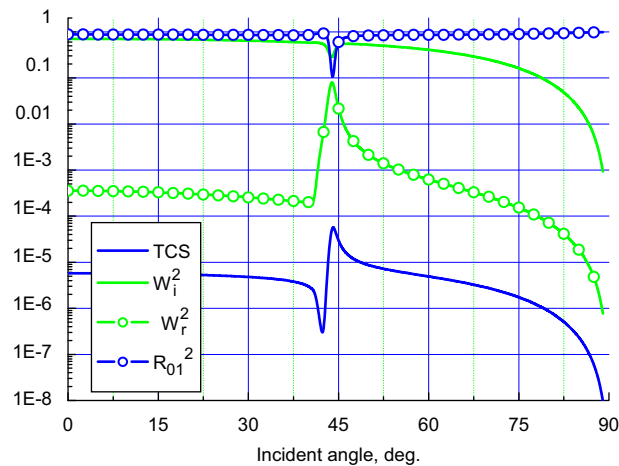


Fig. 9. TCS in comparison with fields amplitudes inside Ag film and the reflection coefficient, P-polarization, $\lambda = 532$ nm.

strict monotone behaviour. In the cases of glass and SiN the curve's behaviour is similar to those in Figs. 3, 5 and 7. At the same time while the magnitude of the TCS changes with varying film materials and wavelengths, the position of the peaks stays the same. This happens because varying the film material does not affect the position of the critical angle, which depends on the refractive indices D_1 and D_0 only. A similar behaviour can be observed for a gold film as well (not shown in this paper).

In Fig. 9 the TCS is shown together with the amplitudes $|w_i^p|^2$ of the plane wave propagating from the interface Σ_1 up and $|w_r^p|^2$ of the plane wave propagating from the interface Σ_f down introduced in (1). Besides, the coefficient of the total reflection the exciting P-polarized plane wave from the layered structure prism–film–air:

$$R_{01}^p(\theta_1) = \frac{r_{1f}^p + r_{f0}^p \exp\{-2ik_f \cos \theta_f d\}}{1 + r_{1f}^p r_{f0}^p \exp\{-2ik_f \cos \theta_f d\}}$$

is presented.

From the results presented in Fig. 9 we can observe that the curves for $|R_{01}^p|^2$ and $|w_i^p|^2$ demonstrate minima at an incidence nearby 44° . At the same time the curve for $|w_r^p|^2$ demonstrates strong correlation with TCS curve. They indicate an increase in values beyond the critical angle and reach their maxima at the same angle nearby 44° . Similar results are valid for Au film (not shown in this paper).

From the last results one can conclude that the effect of extreme transmission is supported by the fact that more energy penetrates into a film in the vicinity of $\theta_1 = 44^\circ$. At the same time the increase in the amplitude of the field propagating down from the air–film border at $\theta_1 = 44^\circ$ consequently leads to a stronger excitation of the hole.

To summarize the presented results, we conclude that the excitation of evanescent waves plays the key role in the effect of extreme transmission of light through a nanohole in a noble-metal film. As it has been shown before, the incident angle where the TCS maximum is achieved does not depend on the hole's diameter and filling [9]. It has been found out that the film material plays an essential role for the effect appearance. Also the effect is more distinct at those wavelengths for which the corresponding spectral maximum of TCS (4) is achieved. These wavelengths depend on the film material only.

4. Conclusion

In this paper the spectral characteristics of light scattering by a nanohole in a metal film on a glass prism have been analysed. It has been shown that the ETE is more distinct at those wavelengths where the corresponding spectral maximum of TCS (4) is achieved. Moreover it was found out that this maximum is reached when the real part of the wavelength depending film permittivity belongs to the range $[-11.5, -10.2]$. This can help to produce an appropriate film material (e.g. noble-metals alloy) enhancing the effect of extreme light transmission. Close correlation between SPR and ETE has been detected. Besides, it has been shown that the excitation of the evanescent waves plays the key role in the ETE. We believe that employing evanescent waves and using the ETE could allow improvement of modern schemes of optical antennas and local biosensors. The main advantage of the use of evanescent waves is absence of transmitted plane wave, which must be accounted for in the case when the propagating waves are used.

Acknowledgements

We gratefully acknowledge funding of this research by Deutsche Forschungsgemeinschaft (DFG) and the Russian Foundation for Basic Research (RFBR).

References

- [1] Ebbesen TW, Lezec HJ, Ghaemi HF, Thio T, Wolff PA. Extraordinary optical transmission through sub-wavelength hole arrays. *Nature* 1998;391:667.
- [2] Wannemacher R. Plasmon-supported transmission of light through nanometric holes in metallic thin films. *Opt Commun* 2001;195:107.
- [3] Genet C, Ebbesen TW. Light in tiny holes. *Nature* 2007;225:39.
- [4] de Abajo FJG. Colloquium: light scattering by particle and hole arrays. *Rev Mod Phys* 2007;79:1267.
- [5] Sönnichsen C, Duch AC, Steininger G, Koch M, von Plessen G, Feldmann J. Launching surface plasmons into nanoholes in metal films. *Appl Phys Lett* 2000;76(210):140.
- [6] Shuford KL, Gray SK, Ratner MA, Schatz GC. Substrate effects on surface plasmons in single nanoholes. *Chem Phys Lett* 2007;435:123.
- [7] Eom GS, Yang D, Lee S, Park S, Lee Y, Hahn JW. Wave propagation characteristics of a figure-eight shaped nanoaperture. *J Appl Phys* 2007;101. 103101-1.
- [8] Yin L, Vasko-Vlasov VK, Rydh A, et al. Surface plasmons at single nanoholes in Au films. *Appl Phys Lett* 2004;85(3):467.
- [9] Eremina E, Eremin Y, Grishina N, Wriedt T. Analysis of light scattering in the evanescent waves area by a cylindrical nanohole in a noble-metal film. *Opt Commun* 2008;281:3581.
- [10] Zayats AV, Smolyaninov II, Maradudin AA. Nano-optics of surface plasmon polaritons. *Phys Rep* 2005;408:131.
- [11] Chew WC. *Waves and fields in inhomogeneous media*. NY: IEEE Press; 1995.
- [12] Colton D, Kress R. *Inverse acoustic and electromagnetic scattering theory*. Berlin: Springer; 1992.
- [13] Eremin YuA. The method of discrete sources in electromagnetic scattering by axially symmetric structures. *J Commun Technol Electron* 2000;45(2): 269.
- [14] Kong JA. *Electromagnetic wave theory*. Cambridge, MA: EMW Publ.; 2000.
- [15] Doicu A, Eremin Yu, Wriedt T. *Acoustic and electromagnetic scattering analysis using discrete sources*. London: Academic Press; 2000.
- [16] Eremin Y, Orlov N, Sveshnikov A. In: Wriedt T, editor. *Generalizes multipole techniques for electromagnetic and light Scattering*. Amsterdam: Elsevier Science; 1999. p. 39.
- [17] Lynch DW, Hunter WR. Comments on the optical constants of metal and an introduction to the data for several metals. In: Palik ED, editor. *Handbook of optical constants of solids 1*. San Diego: Academic Press; 1985.